High-resolution NMR imaging of objects with dipolar-broadened spectra

V. Antochshuk,[1] M.-J. Kim, and A.K. Khitrin*

Department of Chemistry, Kent State University, Kent, OH 44242-0001, USA

Received 23 October 2003; revised 16 December 2003

Abstract

It is shown that, in some substances with dipolar-broadened conventional NMR spectra, it is possible to use long-lived coherent response signals, excited by long and weak radiofrequency pulses, for producing NMR images with high spatial resolution. Compared to other techniques, the method does not require high field gradients or strong radiofrequency fields, and therefore, can be applied to large objects.
© 2003 Elsevier Inc. All rights reserved.

Keywords: NMR imaging; Coherent response; Soft excitation; Liquid crystal; Adamantane

1. Introduction

Magnetic resonance imaging (MRI) and local spectroscopy are among the most powerful techniques for non-destructive study of various objects. MRI is widely used in biological science and medicine for, as an example, producing high quality images of the inside of the human body. The images are reconstructed from Fourier transforms of NMR signals of nuclear spins in the presence of radiofrequency and magnetic field gradient pulses. The achievable spatial resolution Δx in the direction x can be estimated as [1]

$$\Delta x = 2\pi \Delta f / (\gamma G_x), \tag{1}$$

where Δf is the linewidth, G_x is the gradient of magnetic field in x-direction, and γ is the gyromagnetic ratio of the resonant nuclei. As one can see from Eq. (1), for high spatial resolution one needs sharp NMR signals or strong gradients of the magnetic field. NMR lines are very narrow in liquids ($\Delta f \sim 0.1$–10 Hz), where anisotropic dipole–dipole interactions are averaged by fast molecular motions. Most of the MRI applications use NMR spectra of liquids. The achievable spatial resolution is about 0.1 mm for large objects (human body) and up to one micron for small objects (NMR microscopy) [2]. Spatial resolution is proportional to the NMR linewidth. With the existing techniques, the resolution is considerably less for solids or "soft solids" where, in contrast to liquids, dipole–dipole interactions between nuclear spins are not averaged out by fast molecular motions.

Compared to the impressive success of medical applications, MRI use in materials science for imaging solid objects is rather limited. In solids or substances with restricted molecular motions, NMR lines are 3–5 orders of magnitude broader. According to Eq. (1), a corresponding increase in strength of the magnetic field gradients is required for the same level of spatial resolution. However, over the past several years there has been an increased interest in using MRI to examine solid materials or porous media, the objects with broad NMR lines. The main techniques are NMR line-narrowing with multi-pulse sequences [3–5] and use of ultra-strong gradients: stray fields of an NMR magnet [6–8]. Among line-narrowing multi-pulse sequences the ones based on the magic echo [9] are especially convenient for imaging applications [10–12]. The systems with broadened spectra, studied with MRI techniques, include polymers [13–16], porous materials [17,18], and multi-phase systems

[19]. A review of imaging techniques for solid materials can be found in [20]. Despite considerable progress, spatial resolution for solid samples remains much lower than for liquid samples. Besides that, application of the methods mentioned above to large objects faces serious technical problems of creating large gradients and/or high radiofrequency field in a large volume.

Recently, we have found that long and weak radiofrequency pulses can produce long-lived coherent response signals in systems with dipolar-broadened spectra. This novel phenomenon may have interesting practical applications. One of them is using collective dynamics of clusters of coupled spins to store [21] and process in parallel [22] large amounts of information. Another promising application of such coherent response signals could be MRI with greatly improved spatial resolution.

2. Results

Two examples in Fig. 1 demonstrate the line-narrowing which can be achieved by using the new type of excitation of NMR signals. Figs. 1A and C show conventional ^{1}H NMR spectra of 5CB (4′-*n*-pentyl-4-biphenylcarbonitrile) and adamantane, respectively. Their widths are determined by residual dipolar couplings between proton spins. For the liquid crystalline sample of 5CB, with soft excitation, the linewidth is decreased by more than 2000 times (Fig. 1B). Considerable line-narrowing has been also achieved for solid adamantane (Fig. 1D). Actual phases of the signals excited by soft pulses are opposite to those of the conventional spectra. For convenience, the spectra in Figs. 1B and D are shown with 180° phase shifts.

Feasibility of using the long-lived coherent response signals for producing NMR images is demonstrated in Fig. 2, which shows a 1D image of a model object. The phantom is a 5 mm flat-bottomed NMR tube filled with liquid crystal, and there is an axially symmetric Teflon insert inside of the tube. The gradient is applied along the symmetry axis, and the corresponding ^{1}H NMR spectrum reflects distribution of the proton-containing substance (liquid crystal) along this direction. One can see that the total spectral width of the image is an order of magnitude less than the linewidth of conventional NMR spectrum of 5CB. The image is obtained with weak magnetic field gradient of only 0.5 G/cm. This gradient strength is typical for medical MRI scanners. With conventional excitation, three orders of magnitude stronger gradient would be needed to reach comparable spatial resolution. The arrow in Fig. 2 indicates the boundary of sensitive region of the probe.

The phantom in Fig. 3 consists of three layers of powdered solids: adamantane–potassium dichromate–
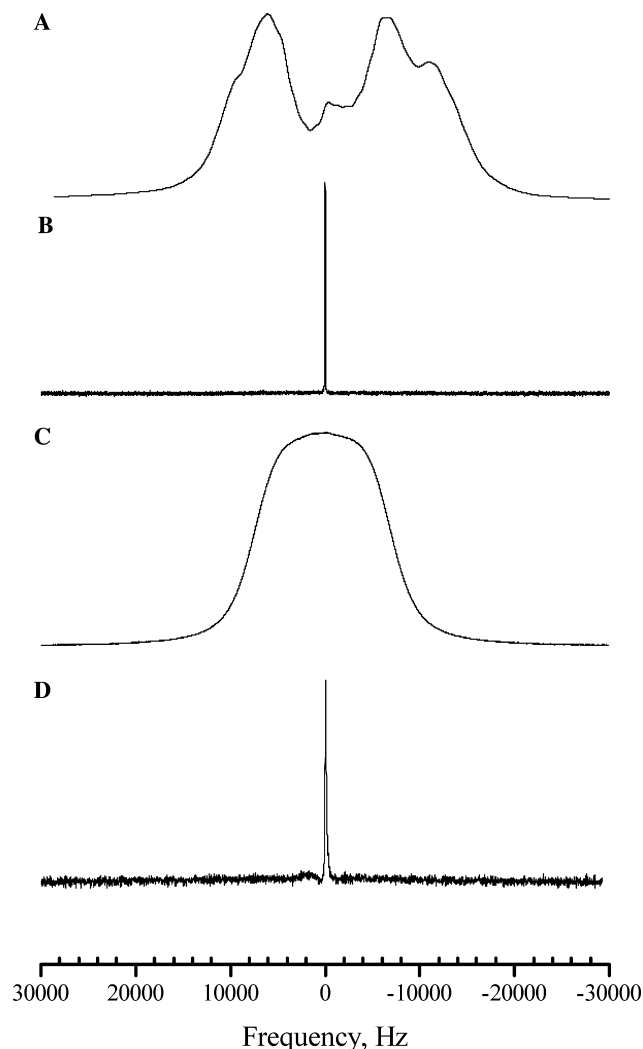

Fig. 1. Conventional ^{1}H NMR spectra of 5CB (A) and adamantane (C) obtained with 3.5 μs 90° pulse; (B) spectrum of 5CB excited with soft 0.2 s pulse with RF amplitude $\gamma B_1/2\pi = 15$ Hz, acquisition delay was 1 ms, the linewidth is 23 Hz; and (D) spectrum of adamantane excited with soft 12 ms pulse with RF amplitude $\gamma B_1/2\pi = 60$ Hz, acquisition delay was 200 μs, the linewidth is 120 Hz.

adamantane. The powders have been packed into a 5 mm flat-bottomed NMR tube. Proton density distribution along the symmetry axis (1D image) shown in Fig. 3 has been obtained with the same gradient of only 0.5 G/cm. Similar to the 5CB phantom, the total spectral width of the image is considerably less than the width of the conventional NMR spectrum (Fig. 1C).

3. Experiment

The experiments were carried out with a Varian Unity/Inova 500 MHz NMR spectrometer equipped with a *z*-gradient probe. 5CB and adamantane were purchased from Aldrich and used without further purification. To compensate for a finite rise time of the
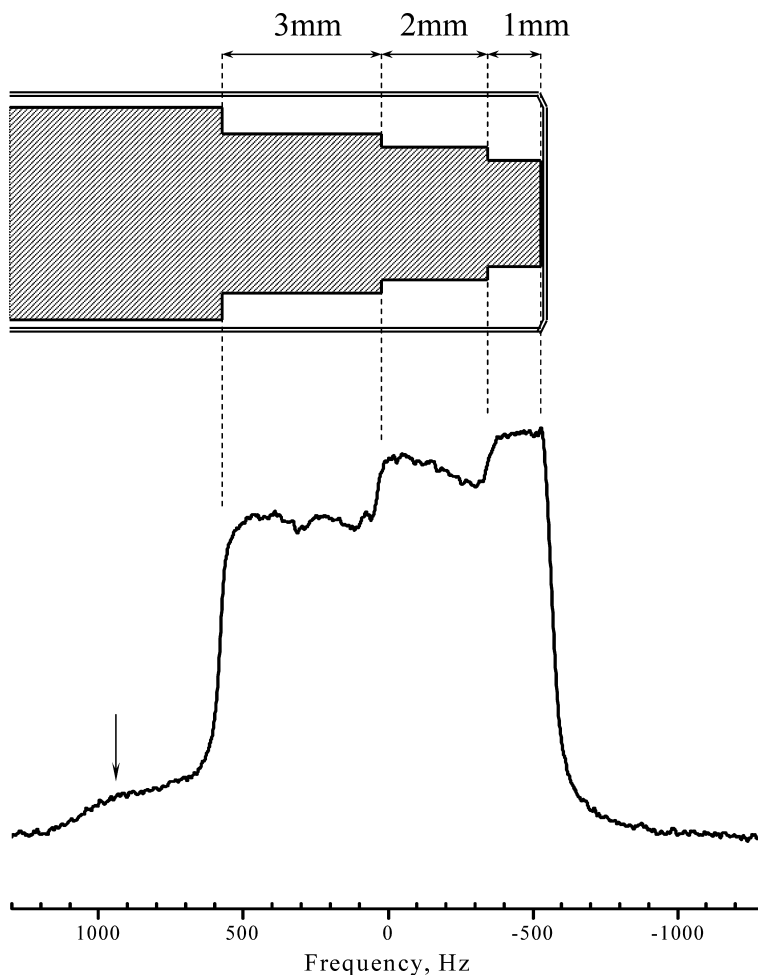
Fig. 2. 5CB phantom and 1D image. The excitation pulse parameters are the same as in Fig. 1B, the gradient is 0.5 G/cm, the number of transients is 5000.

magnetic field gradient, a gradient echo has been used. After the RF excitation pulse, to obtain the image of 5CB phantom (Fig. 2), a negative gradient of 1 G/cm and a duration of 80 μs have been applied and the acquisition gradient of 0.5 G/cm followed after 600 μs delay. For the imaging of adamantane phantom (Fig. 3), a negative gradient of 1.25 G/cm and a 40 μs duration have been applied, and the 0.5 G/cm acquisition gradient followed after 120 μs delay. The first point of FID for Fourier transform was the point of maximum amplitude of the FID signal.

4. Discussion

Soft excitation of long-lived response signals does not offer a universal solution for solid-state NMR imaging. In many cases, the signals are too weak to be practically used for imaging. The presence of internal molecular motions is favorable for stronger response signals (B.M. Fung, V.L. Ermakov, "The presence of long-lived spin states in organic solids with rapid molecular motions," to be published) and we expect that the technique will be most useful for imaging "soft" solids with intense anisotropic molecular motions. Integral intensity of the sharp peaks is always much smaller than that of conventional NMR spectra. However, in favorable cases, like liquid crystals or some "soft" polymers, the peak height can be comparable to that of conventional spectrum. Since much smaller gradients are needed for the same spatial resolution, we can expect considerable improvement of the S/N ratio compared to imaging with conventional excitation of signals. In organic solids, the coherent response signals are usually weak. As an example, the height of the peak for adamantane in Fig. 1D is only 0.2% of the signal excited by a hard 90° pulse. In this case, the sensitivity is decreased even compared to the single point imaging (SPI). Poor sensitivity can be partially compensated by faster repetition of the acquisition cycles. Similar to the FLASH technique [23], which uses pulses with small flip angles, each weak pulse produces only a small
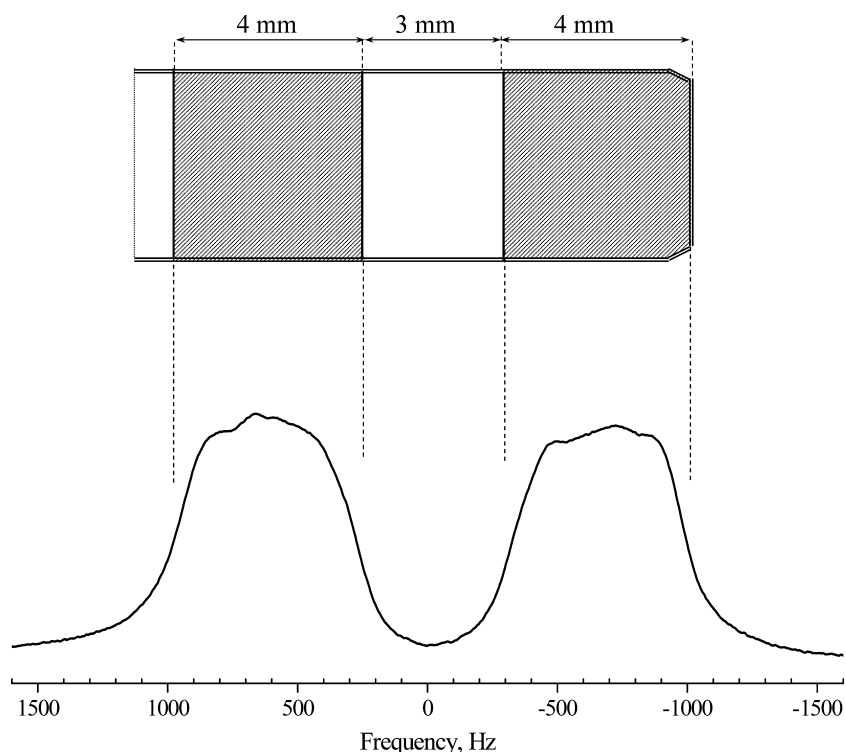
Fig. 3. Adamantane phantom and 1D images. The excitation pulse parameters are the same as in Fig. 1D, the gradient is 0.5 G/cm, and the number of transients is 5000.

change of the total z-component of magnetization and, therefore, acquisitions can follow much faster than T_1.

The use of long-lived coherent response signals can significantly decrease the strength of gradients needed to achieve a desired spatial resolution, and the RF power during "soft" excitation is extremely small. This makes this technique more suitable for imaging large objects. Another advantage comes from using the generator frequency rather than the Larmor frequency for labeling spatial position: there are no distortions caused by a static field inhomogeneity (magnetic susceptibility variations or non-perfect shims) and the schemes for compensating such distortions [24] are not necessary. In the presence of inhomogeneous static field, different regions of a broad spectrum are excited in different parts of a sample but the frequency of the excited signal is the same. Applied gradients shift this common precession frequency. In addition, there is no distortion arising from the interaction between radiofrequency pulses and gradient pulses [25].

Acknowledgments

References

[1] P.T. Callaghan, Principles of Nuclear Magnetic Resonance Microscopy, Clarendon Press, Oxford, 1991.

[2] S.-C. Lee, K. Kim, J. Kim, S. Lee, J.H. Yi, S.W. Kim, K.-S. Ha, C. Cheong, One micrometer resolution NMR microscopy, J. Magn. Reson. 150 (2001) 207–213.

[3] P. Mansfield, P.K. Grannell, "Diffraction" and microscopy in solids and liquids by NMR, Phys. Rev. B 12 (1975) 3618–3634.

[4] D.G. Cory, J.B. Miller, A.N. Garroway, Time-suspension multiple-pulse sequences: applications to solid-state imaging, J. Magn. Reson. 90 (1990) 205–213.

[5] D.E. Demco, B. Blümich, Solid-state NMR imaging methods. Part II: Line narrowing, Concepts Magn. Reson. 12 (2000) 269–288.

[6] J.H. Iwamiya, S.W. Sinton, Stray-field magnetic resonance imaging of solid materials, Solid State NMR 6 (1996) 333–345.

[7] M.J.D. Mallett, M.R. Halse, J.H. Strange, Stray field imaging by magnetic field sweep, J. Magn. Reson. 132 (1998) 172–175.

[8] D.E. Demco, B. Blümich, Solid-state NMR imaging methods. Part I: Strong field gradients, Concepts Magn. Reson. 12 (2000) 188–206.

[9] W.-K. Rhim, A. Pines, J.S. Waugh, Time-reversal experiments in dipolar-coupled spin systems, Phys. Rev. B 3 (1971) 684–696.

[10] S. Matsui, M. Nonaka, T. Nakai, T. Inouye, Magic echo solid-state NMR imaging without a rapidly switchable field gradient, J. Magn. Reson. 138 (1999) 220–224.

[11] S. Matsui, S. Saito, Symmetric echo acquisition for absolute-value display in solid-state NMR imaging, J. Magn. Reson. 149 (2001) 103–109.

[12] D.E. Demco, B. Blümich, NMR imaging of materials, Curr. Opin. Solid State Mater. Sci. 5 (2001) 195–202.

[13] P. Baras, I. Seimenis, P. Kipouros, P. Papagiannis, A. Angelopoulos, L. Sakellious, E. Pappas, D. Baltas, P. Karaiskos, P.

Sandilos, L. Vlachos, Polymer gel dosimetry using a three-dimensional MRI acquisition technique, Med. Phys. 29 (2002) 2506–2516.

[14] M. Knörgen, K.-F. Arndt, S. Richter, D. Kuckling, H. Schneider, Investigation of swelling and diffusion in polymers by ^{1}H-NMR imaging: LCP networks and hydrogels, J. Mol. Struct. 554 (2000) 69–79.

[15] P. Adriaensens, A. Pollaris, D. Vanderzande, J. Gelan, J.L. White, A.J. Dias, M. Kelchtermans, Critical analysis of network defects in cross-linked isobutylene-based elastomers by NMR imaging, Macromolecules 32 (1999) 4692–4699.

[16] S. Ganapathy, P.R. Rajamohanan, M.V. Badiger, A.B. Mandhare, R.A. Mashelkar, Proton magnetic resonance imaging in hydrogels: volume phase transition in poly(N-isopropylacrylamide), Polymer 41 (2000) 4543–4547.

[17] P. Szomolanyi, D. Goodyear, B. Balcom, D. Matheson, SPIRAL-SPRITE: a rapid single point MRI technique for application to porous media, Magn. Reson. Imaging 19 (2001) 423–428.

[18] Z. Fang, D. Hoepfel, K. Winter, Application of single point Imaging (SPI) to solid state materials, Magn. Reson. Imaging 19 (2001) 501–503.

[19] S.D. Beyea, S.A. Altobelli, L.A. Mondy, Chemically selective NMR imaging of a 3-component (solid–solid–liquid) sedimenting system, J. Magn. Reson. 161 (2003) 198–203.

[20] J.B. Miller, NMR imaging of materials, Prog. Nucl. Magn. Reson. Spectrosc. 33 (1998) 273–308.

[21] A.K. Khitrin, V.L. Ermakov, B.M. Fung, Nuclear magnetic resonance molecular photography, J. Chem. Phys. 117 (2002) 6903–6906.

[22] A.K. Khitrin, V.L. Ermakov, B.M. Fung, NMR implementation of parallel search algorithm, Phys. Rev. Lett. 89 (2002) (277902-1/ 4).

[23] A. Haase, J. Frahm, D. Matthaei, W. Hänicke, K.-D. Merboldt, FLASH imaging. Rapid NMR imaging using low flip-angle pulses, J. Magn. Reson. 67 (1986) 258–266.

[24] J.B. Miller, A.N. Garroway, Removal of static field inhomogeneity and chemical-shift effects in NMR imaging, J. Magn. Reson. 67 (1986) 575–579.

[25] D.G. Cory, Distortions in multiple-pulse solid state NMR imaging: gradient decoupling, time-sequenced second averaging, and over-sampling, Solid State NMR 6 (1996) 347–355.